# Measurement and Simulation of Reflector Antenna

L.J.Foged , M.A. Saporetti , M. Sierra-Castanner , E. Jørgensen , T. Voigt , F. Calvano , D. Tallini

***Abstract*— Well-established procedures are consolidated to determine the associated measurement uncertainty for a given antenna and measurements scenario [1-2]. Similar criteria for establishing uncertainties in numerical modelling of the same antenna are still to be established. In this paper, we investigate the achievable agreement between antenna measurement and simulation when external error sources are minimized. The test object, is a reflector fed by a wideband dual ridge horn (SR40-A and SH4000). The highly stable reference antenna has been selected to minimize uncertainty related to finite manufacturing and material parameter accuracy. Two frequencies, 10.7GHz and 18GHz have been selected for detailed investigation.**

**The antenna has been measured in two reference spherical near-field measurement facilities as a preparatory activity for a Facility Comparison Campaign on this antenna in the frame of a EurAAP/WG5 activity. A full CAD model, in step compatible format, has been provided and the antenna has been simulated using different numerical methods from different software vendors [4-7]. Each participant was responsible for generating a suitable mesh and the numerical stability of their solution.**

***Index Terms*—antenna, measurement, simulation, numerical methods.**

## I. Test Object

The SR40-A and SH4000 antenna is shown in Fig. 1. The SR40-A is an offset parabolic reflector, precision machined from a single block of aluminum. The circular interface with precision holes allows the user to center the antenna with very high accuracy. The alignment accuracy is determined to within ±0.01°. The SH4000 wide band Dual Ridge Horn is a highly stable reference antenna. The antenna is precision fitted to the mounting bracket of the reflector.

This antenna is selected as test object in a comprehensive measurement facility comparison activity as a EurAAP Working Group 5, activity.

## II. Measurement Campaign

Comparative measurements based on high accuracy reference antennas and involving different antenna measurement systems are important instruments in the evaluation, benchmarking and calibration of the measurement facilities. Regular inter comparisons are also an important instrument for traceability and quality maintenance. These activities promote and document the measurement confidence level among the participants and are an important prerequisite for official or unofficial certification of the facilities.

Different European facility comparison campaigns, have been completed during the last years in the framework of different European Activities: Antenna Measurement Activity of the Antenna Centre of Excellence-VI UE Frame Program; COST ASSIST, IC0603 and COST-VISTA, IC1102.

Activities related to facility comparisons are now included in the Antenna Measurement, Working Group 5 Activity of EurAAP, where a specific on-going task for Antenna Measurement Intercomparison has been approved.

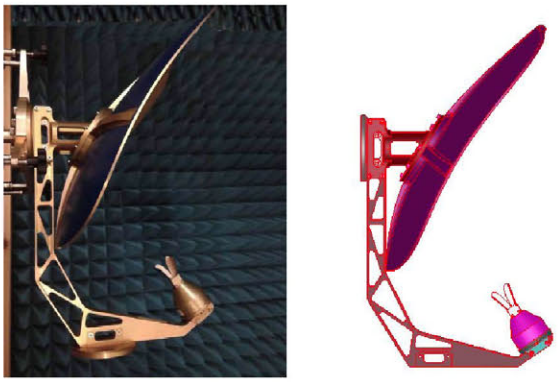

Fig. 1. Reflector SR 40-A fed by SH4000 Dual Ridge Horn: Antenna during measurement (Left); CAD file for simulation (Right).

### A. *Test Plan and Participating Facilities*

The measured SR40-A and SH4000 antenna is part of a currently ongoing larger measurement facility comparison campaign within a EurAAP Working Group 5 activity. Two spherical Near Field ranges, Technical University of Madrid (UPM), Spain and SATIMO SG 64 (MVG), France, have contributed to the reference measurements reported here. The measurements data requested for the facility comparison campaign are reported in TABLE I. A full list of information required from each participating facility, for the post processing and the comparison of data, is reported in [3].

TABLE I. MEASUREMENT DATA, REFLECTOR SR 40-A FED BY SH4000 DUAL RIDGE HORN

| | | |
|---|---|---|
| **Full 3D Gain Measurement** | Frequency Range | 10.7, 12.6, 14.5,18, 19, 20, 28, 29, 30, 31 ,33, 38 GHz |
| | Phi | From 0° to 135°(45° step) |
| | Theta | From -180° to 180° (1° step) |
| | Ports (K type female connectors) | Measurement: vertical polarization |

### B. *Determination of Measured Reference Pattern*

The access to measured data from different facilities in good agreement between them, increase the confidence level of the measured data.

In [3], different data processing procedures have been investigated to derive reference patterns with increased confidence level based on measurements in different facilities. The reference pattern can be calculated as the simple mean or weighted mean of each measured data point where the weights are proportional to the estimated uncertainty. The uncertainty associated with the mean is "improved" if the measurements can be considered truly independent.

For this activity, considering the availability of three sets of measurements data from UPM and MVG facilities, the simple mean of the radiation pattern, using amplitude data only, has been used to define the reference pattern.

## III. SIMULATION CAMPAIGN

Simulations have been performed at 10.7GHz and 18GHz, considering the nominal dimensions of the feed and reflector and ignoring finite manufacturing and material parameter accuracy. The electrical conductivity of aluminum was assumed to 3.56 $10^7$ S/m in the simulation of ohmic losses. The complete CAD file of the antenna was provided to each of the participants involved. Each participant was responsible for generating a suitable mesh and the numerical stability of their solution. The information collected from simulations is reported below:

- Peak directivity at 10.7 and 18 GHz;
- Directivity patterns in 4 cuts (Ludwig III[8] Co/Cx 0º, 45º, 90º & 135º) -180º to 180º in 1º and 0.1º step;
- Return loss;
- Ohmic losses;
- Description of numerical method (with illustration – Ex: currents on reflector, grid used etc).

### A. *GRASP (TICRA)*

GRASP offers a variety of analysis methods suitable for electrically large scattering and radiation problems such as reflector antennas and satellite platforms. The method used here is a frequency domain higher-order Method of Moments surface integral equation solver using curved mesh elements up to 2λ by 2λ. The solution is accelerated by a recently introduced Multi-level Fast Multipole Method (MLFMM) developed particularly for higher-order discretizations [14]. The new HO-MLFMM solver has been further enhanced with the ability to work with non-connected meshes, which provides increased robustness in practical applications. For the present problem, the fine details of the feed was modelled with tiny patches (0.01 λ) whereas the reflector surface was modelled with large patches (2λ). The surface current was then expanded in polynomials between 1st and 9th order depending on the electrical size of each patch. The MLFMM solver includes an efficient preconditioner that enables fast convergence while being rather insensitive to the presence of small geometrical details or the use of high polynomial orders. For the present 18 GHz example, a relative solution error of 0.001 was reached after 20 iterations. The currents induced on the antenna structure, as well as the mesh used in the computations, are shown in Fig.2.

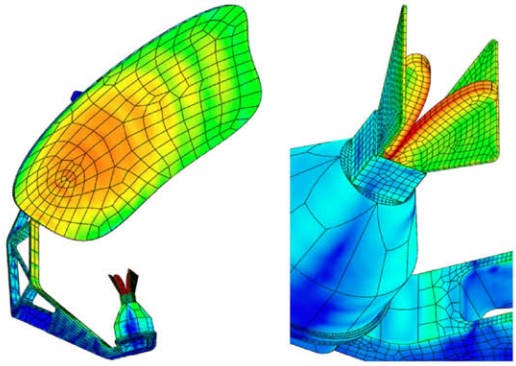

Fig. 2. GRASP currents induced on the antenna and mesh grid @18GHz. Reflector SR 40-and SH4000 fed (Left), Close-up of the feed (Right).

### B. *HFSS (ANSYS)*

The currents induced on the structure for the present problem at 10.7GHz and 18GHz are shown in Fig. 3.

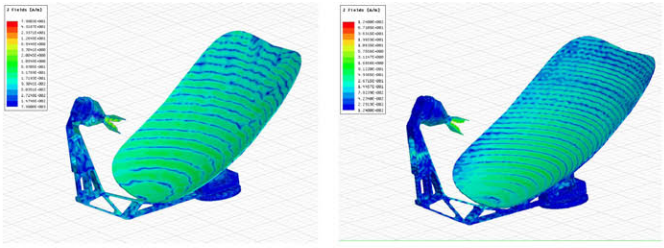

Fig. 3. HFSS simulated surface current density Js@10.7GHz (Left) and 18GHz (Right) Reflector SR 40-A with SH4000 Dual Ridge Horn.

The hybrid FEBI [9] is a powerful new enhancement to the FEM [13] solver available in HFSS. This new technique gives the design engineer the advantages of an FEM simulation with the efficiency and accuracy of an IE solution for open boundary problems. This procedure is accurate for conformal, concave and/or separate air volumes, allowing users to reduce the size of the FEM solution region resulting in a significant reduction in the solution time and the amount of memory required to solve the problem.

### C. *FEKO*

FEKO is a comprehensive electromagnetic software suite (now part of Altair's HyperWorks CAE simulation software platform), which includes many frequency and time domain solvers to solve a wide set of problems, involving complex materials and electrically large objects. FEKO has two sets of methods (full-wave methods and asymptotic methods), which are also hybridized to take profit from the advantages of both. The method used for this problem is FEKO's MLFMM, which was included in FEKO in 2004. Alternatively, and to cross-validate the results, one could also use for this problem domain decomposition: first using MLFMM for the feeder and afterwards use such results as source while modelling the reflector with Physical Optics (PO). The currents induced on the antenna structure and the mesh grid used @ 18GHz are shown in Fig. 4.

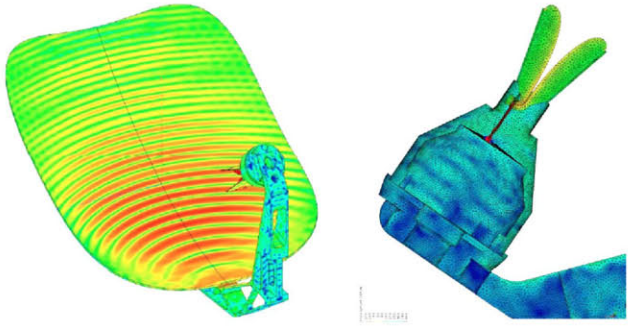

Fig. 4. FEKO currents induced on the antenna structure and applied mesh @18GHz on the Reflector SR 40-A with SH4000 Dual Ridge Horn. Currents (Left); Close-up of the feed (Right).

### D. *CST STUDIO SUITE (CST)*

CST offers several numerical simulation methods which are very efficient for reflector design. Given the frequencies and the electrical size of the reflector (24 λ x 28 λ @ 18 GHz), all the provided results have been obtained in a single simulation run using the Time Domain Solver based on the Finite Integration Technique (FIT). Perfect Boundary Approximation (PBA) is used for the spatial discretization of the structure. The simulated structure and the electromagnetic fields are mapped to a hexahedral mesh. PBA allows a very good approximation of even curved surfaces within the cubic mesh cells. The obtained E-field for the present problem@10.7GHz and 18GHz is shown in Fig. 5.

The results can be cross-checked using a hybrid approach in which an equivalent NF source from measurements or generated by a time domain simulation of the horn antenna can be used as an excitation source. The simulation of the reflector can be performed by the Integral Equation solver based on MLFMM or the Asymptotic Solver based on the Shooting and Bouncing Ray (SBR) method. Farfield results, generated using this approach, agree very closely with the full time domain simulation pattern.

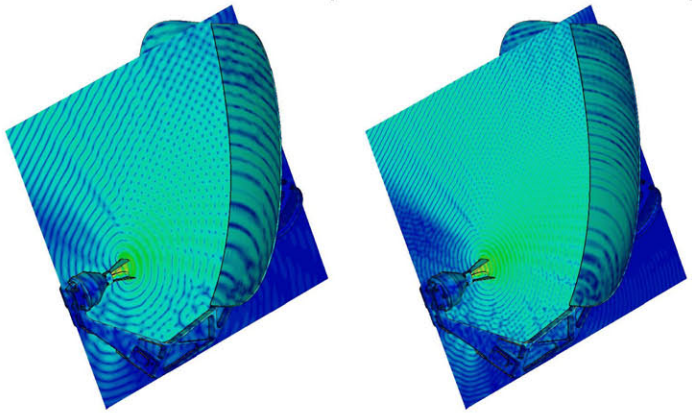

Fig. 5. CST Simulated E-field @10.7GHz (Left) and @18GHz (Right). Reflector SR 40-A with SH4000 Dual Ridge Horn.

## IV. Comparison Results

The simulations, based on different numerical methods are generally in very good agreement when compared to each other. The agreement between simulation and measurements is also considered excellent when considering uncertainties due to measurement and manufacturing. In the following, comparisons including the peak directivity, patterns, equivalent error level and losses are reported.

### A. *Peak directivity comparison*

The peak directivity values are reported for measurements and simulations in TABLE II. The table confirms the very good agreement between measurements and simulations.

TABLE II. Measured and Simulated Peak Directivity

| **Peak Directivity [dBi]** | | | | | |
|---|---|---|---|---|---|
| **Frequency** | ***Meas*** | ***CST*** | ***FEKO*** | ***GRASP*** | ***HFSS*** |
| ***10.7 GHz*** | 30.99 | 30.96 | 31.11 | 31.09 | 31.04 |
| ***18 GHz*** | 35.30 | 35.69 | 35.56 | 35.59 | 35.53 |

### B. *Pattern comparison*

The co-polar and cross-polar components at four patterns cuts, phi=0°, 45°, 90° and 135° @ 10.7GHz and 18GHz are compared with measurements in Fig. 6 to Fig. 13. MEAS is the measured reference as the mean of three measurements performed at UPM and MVG. The simulated results are from GRASP, FEKO, CST and HFSS.

The agreement between simulation and measurements in the plots is good especially considering that simulation results have been plotted with 0.1° angular step, while the step for measurements is 1°.

The agreement can also be evaluated as a single value. The pattern correlation or equivalent noise level [3] is reported in the following paragraph.

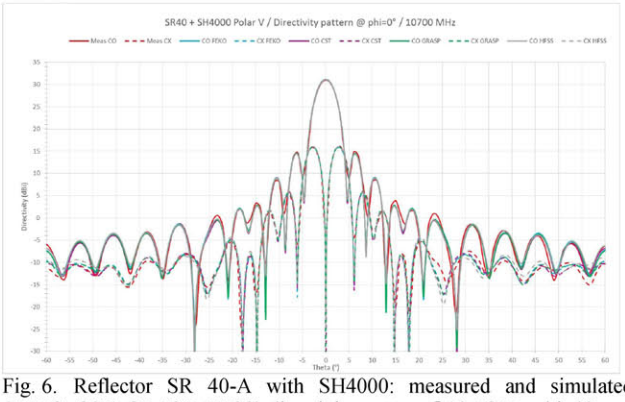


Fig. 6. Reflector SR 40-A with SH4000: measured and simulated (FEKO, CST, GRASP, HFSS) directivity pattern @10.7GHz, phi=0°.

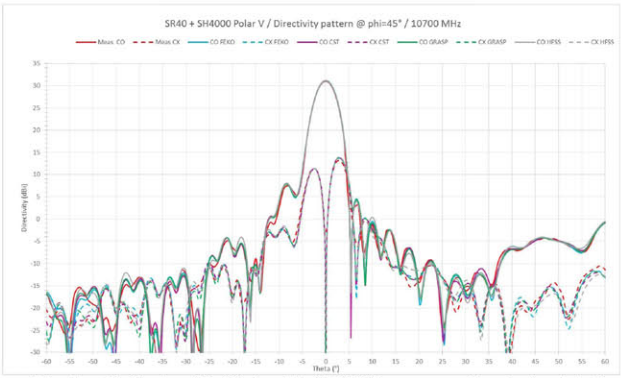


Fig. 7. Reflector SR 40-A with SH4000: measured and simulated (FEKO, CST, GRASP, HFSS) directivity pattern @10.7GHz, phi=45°.

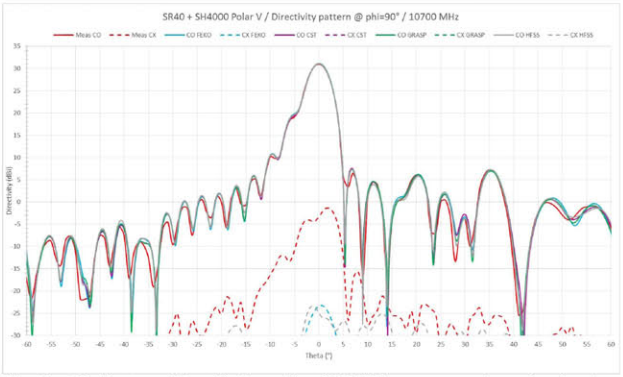


Fig. 8. Reflector SR 40-A with SH4000: measured and simulated (FEKO, CST, GRASP, HFSS) directivity pattern @10.7GHz, phi=90°.

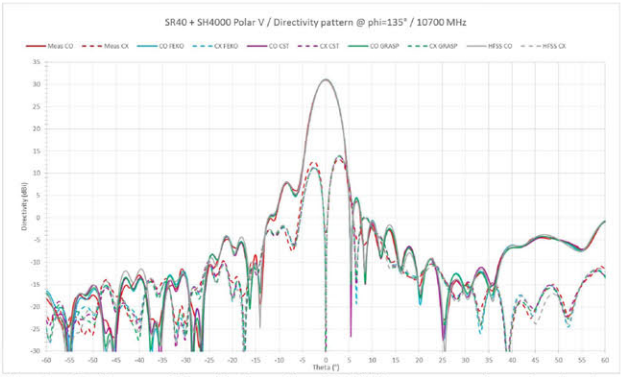


Fig. 9. Reflector SR 40-A with SH4000: measured and simulated (FEKO, CST, GRASP, HFSS) directivity pattern @10.7GHz, phi=135°.

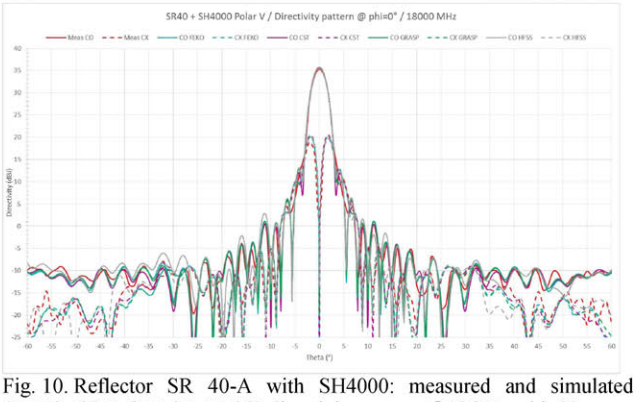


Fig. 10. Reflector SR 40-A with SH4000: measured and simulated (FEKO, CST, GRASP, HFSS) directivity pattern @18GHz, phi=0°.

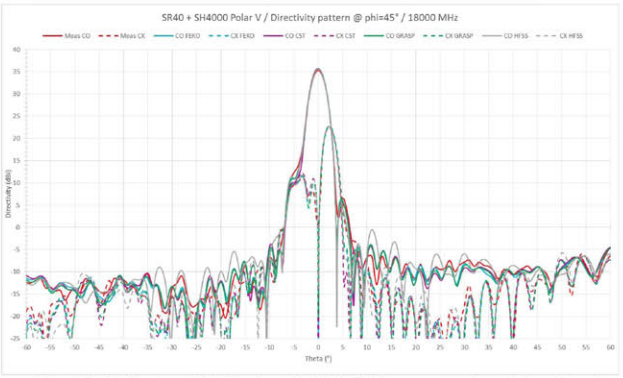


Fig. 11. Reflector SR 40-A with SH4000: measured and simulated (FEKO, CST, GRASP, HFSS) directivity pattern @18GHz, phi=45°.

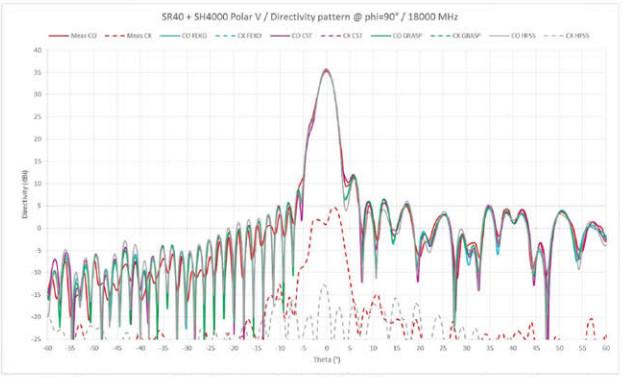


Fig. 12. Reflector SR 40-A with SH4000: measured and simulated (FEKO, CST, GRASP, HFSS) directivity pattern @18GHz, phi=90°.

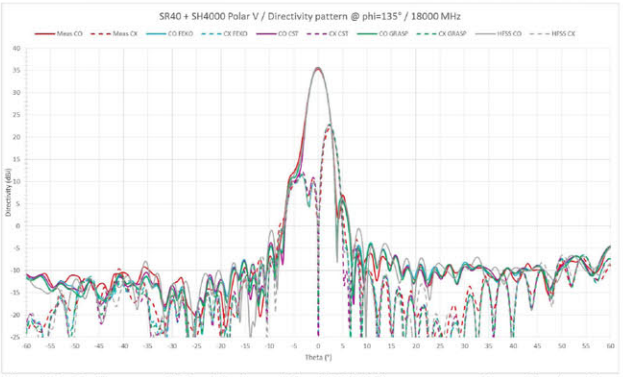


Fig. 13. Reflector SR 40-A with SH4000: measured and simulated (FEKO, CST, GRASP, HFSS) directivity pattern @18GHz, phi=135°.

### C. Pattern Correlation / Equivalent Noise Level

The visible pattern agreement is confirmed by computing the pattern correlation or equivalent noise level [3]. Correlation of simulation and measurement has been computed in a ±20° conical angle for both polarizations as reported in TABLE III. Correlation values of ~40dB are similar to what has been achieved in recent measurement comparisons [3].

TABLE III. EQUIVALENT NOISE LEVEL@10.7 AND 18 GHZ

| **Equivalent Noise Level wrt Measurements [dB] @10.7 GHz** | | | | | | | | |
|---|---|---|---|---|---|---|---|---|
| **Phi** | ***CST*** | | ***FEKO*** | | ***GRASP*** | | ***HFSS*** | |
| | *CO* | *CX* | *CO* | *CX* | *CO* | *CX* | *CO* | *CX* |
| ***0°*** | -42.52 | -48.20 | -42.07 | -48.09 | -43.57 | -48.86 | -44.05 | -48.47 |
| ***90°*** | -44.08 | -43.24 | -42.41 | -43.86 | -43.91 | -43.22 | -44.73 | -43.38 |
| **Equivalent Noise Level wrt Measurements [dB]@18 GHz** | | | | | | | | |
| **Phi** | ***CST*** | | ***FEKO*** | | ***GRASP*** | | ***HFSS*** | |
| | *CO* | *CX* | *CO* | *CX* | *CO* | *CX* | *CO* | *CX* |
| ***0°*** | -41.61 | -42.70 | -41.74 | -44.94 | -41.47 | -44.84 | -43.12 | -44.40 |
| ***90°*** | -39.18 | -42.33 | -40.57 | -42.36 | -40.21 | -42.22 | -40.56 | -42.29 |

### D. Dissipation Loss Comparison

The measured and simulated dissipation losses are reported in TABLE IV. Measured losses are obtained as the difference between the IEEE Gain and the Directivity, therefore the accuracy is related to the gain accuracy of the measurement facilities.

All simulations give similar dissipation estimates. It seems that simulations slightly underestimate the losses. A plausible explanation is connector losses, not included in the simulation scenarios and the uncertainty of the aluminum electrical conductivity considered in the simulations. The vendor sheet value has been used in the simulation with no experimental verification.

TABLE IV. DISSIPATION LOSS

| **Dissipation Loss [dB]** | | | | | |
|---|---|---|---|---|---|
| **Frequency** | ***Meas*** | ***CST*** | ***FEKO*** | ***GRASP*** | ***HFSS*** |
| ***10.7 GHz*** | -0.27 | -0.11 | -0.09 | -0.08 | -0.07 |
| ***18 GHz*** | -0.34 | -0.14 | -0.11 | -0.11 | -0.34 |

### E. Matching / Return Loss Comparison

The measured and simulated return loss values are reported in TABLE V. There are visible differences between simulations and measurements. These can be explained from the difference in matching condition in the simulation scenario and actual antenna. Simulations have been performed considering a discrete excitation port of the SH4000 with definitions depending on the numerical tool. Measurements are referred to a 50Ω high precision connector. The availability, of the return loss, as a curve over the frequency band, instead of two discrete points would probably have been more meaningful for the comparison.

TABLE V. RETURN LOSS

| **Return Loss [dB]** | | | | | |
|---|---|---|---|---|---|
| **Frequency** | ***Meas*** | ***CST*** | ***FEKO*** | ***GRASP*** | ***HFSS*** |
| ***10.7 GHz*** | -12.87 | -13.95 | -9.41 | -12.30 | -12.60 |
| ***18 GHz*** | -17.27 | -14.34 | -15.04 | -16.70 | -14.00 |

## V. CONCLUSIONS

The achievable agreement between antenna measurement and numerical simulation has been investigated. The experiment has been designed to minimize error sources not pertinent to simulation/measurement.

The simulations, based on different numerical methods are generally in very good agreement when compared to each other. The agreement between simulation and measurements is deemed excellent, considering uncertainties due to simulation, measurement and manufacturing. The level of correlation between measurements and simulation achieved here are better than what has been found in recent facility comparisons campaigns. Very good agreement has been achieved for performance parameters such as peak directivity, pattern, and gain contributions such as dissipation loss and matching.

## REFERENCES


[1] ANSI/IEEE Std 149-1979, "Standard Test Procedures for Antennas"

[2] IEEE Std 1720-2012, "Recommended Practice for Near-Field Antenna Measurements".

[3] L. J. Foged, M. Sierra Castañer, L. Scialacqua "Facility Comparison Campaigns within EurAAP", 5th European conference on Antennas and propagation, EuCAP2011, Rome, April 2011.

[4] www.cst.com, CST STUDIO SUITE™, CST AG, Germany

[5] www.feko.info, Altair Engineering GmbH, Germany

[6] www.ansys.com/Products/Simulation+Technology/Electronics/Signal+Intergrity/ANSYS+HFSS, ANSYS Inc. USA

[7] www.ticra.com, Denmark

[8] A.C. Ludwig, "The Definition of CrossPolarization", IEEE Trans. Antennas Propagation, vol. AP-21 no.1, pp. 116-119, Jan. 1973.

[9] X. Yuan, "Three-dimensional Electromagnetic Scattering from Inhomogeneous Objects by the Hybrid Moment and Finite Element Method," IEEETransactions on Microwave Theory and Techniques, Vol. 38, No. 8, August 1990, pp. 1053-1058.

[10] W. C. Chew, J. M. Jin, E. Michielssen, and J. M. Song, Fast and Efficient Algorithms in Computational Electromagnetics, Artech House, Boston, MA, 2001.

[11] Poggio, A. J. and Miller, E. K., "Integral Equation Solutions of Three-Dimensional Scattering Problems." Computer Techniques for Electromagnetics, edited R. Mittra, Pergamon Press, New York, 1973

[12] M. Sabbadini, G. Guida, M. Bandinelli,The Antenna Design Framework ElectroMagnetic Satellite, IEEE Antennas and Prop. magazine 05/2009

[13] J. Jin, The Finite Element Method in Electromagnetics, Second Edition, John Wiley & Sons Inc., New York, NY, 2002.

[14] O. Borries, P. Meincke, E. Jørgensen, and P. C. Hansen, "Multilevel Fast Multipole Method for Higher-Order Discretizations," IEEE Transactions on Antennas and Propagation, vol. 62, no. 9, pp. 4695–4705, Sep. 2014.

[15] T. Weiland: "RF & Microwave Simulators - From Component to System Design" Proceedings of the European Microwave Week (EUMW 2003), München, Oktober 2003, Vol. 2, pp. 591 - 596.

[16] B. Krietenstein, R. Schuhmann, P. Thoma, T. Weiland: "The Perfect Boundary Approximation Technique facing the big challenge of High Precision Field Computation" Proc. Of the XIX International Linear Accelerator Conference LINAC, Chicago, USA, 1998, pp. 860-862.

[17] D. Reinecke, P. Thoma, T. Weiland: "Treatment of thin, arbitrary curved PEC sheets with FDTD" IEEE Antennas and Propagation, Salt Lake City, USA, 2000, p. 26.

[18] L.J. Foged, L. Scialacqua, F. Saccardi, F. Mioc, D. Tallini, E. Leroux, U. Becker, J. L. Araque Quijano, G. Vecchi: "Bringing Numerical Simulation and Antenna Measurements Together", EuCAP2014, The Hague, The Nederlands, April 2014.